Supporting Information

High-Performance Cobalt-Free Perovskite Cathode for Intermediate-Temperature Solid-Oxide Fuel Cells

Yingjie Niu,[†] Wei Zhou,*[,‡] Jaka Sunarso,[‡] Lei Ge,[‡] Zhonghua Zhu,[‡] and Zongping Shao*[,†]

State Key Laboratory of Materials-Oriented Chemical Engineering, College of Chemistry & Chemical Engineering, Nanjing University of Technology, No. 5 Xin Mofan Road, Nanjing 210009, PR China and School of Chemical Engineering, The University of Queensland, Brisbane, Queensland 4072, Australia

RECEIVED DATE (automatically inserted by publisher); E-mail: wei.zhou@uq.edu.au; shaozp@njut.edu.cn

Experimental

$Bi_{0.5}Sr_{0.5}FeO_{3-\delta}$ (BSF) and $La_{0.5}Sr_{0.5}FeO_{3-\delta}$ (LSF) powders were synthesized by a combined EDTA-citrate complexing process. Stoichiometric amounts of $Bi(NO_3)_3{\cdot}5H_2O$ (99.99+%, Sigma-Aldrich), $Sr(NO_3)_2$ (99.9+%, Ajax Finechem Australia) and $Fe(NO_3)_3{\cdot}9H_2O$ (99.9+%, Sigma-Aldrich) were mixed in deionized water and heated at 80°C. Dissolution of $Bi(NO_3)_3{\cdot}5H_2O$ was performed by adding the required amount of HNO_3 (67%, Sigma-Aldrich). EDTA (99.4+%, Ajax Finechem Australia) and citric acid (99.5%, Fluka) were then added as the metal ions' complexing agents. The molar ratio of total metal ions, EDTA and citric acid in the solution was 1:1:2. To ensure complete complexation, solution pH was adjusted to 6 by adding NH_3 aqueous solution (28%, Ajax Finechem Australia). The final powders were obtained from the solution after water evaporation at 90°C to form a transparent gel followed by prefiring of this gel at 250°C and its calcination at 950°C for 5 hours in air.

The crystal structures of the BSF and LSF powders were determined by x-ray diffraction (XRD, Bruker AXS D8 Advance) with filtered Cu-Kα radiation at 40 kV and 40 mA and a receiving slit of 0.2-0.4 mm. The diffraction patterns were collected at room temperature by step scanning in the range of $10^o \leq 2\theta \leq 90^o$ with the scan rate of 2^o min^{-1}. Rietveld refinements on the XRD patterns were carried out using DIFFRAC*plus* Topas 4 software.[1] All initial parameters for structures were taken from ICSD#92335 ($SrFeO_3$) for BSF and ICSD#78066 ($La_{0.5}Sr_{0.5}FeO_3$) for LSF.[2] During refinements, general parameters, such as the scale factor, background parameters and the zero point of the counter were optimized. Profile shape calculations were carried out using the Thompson-Cox-Hastings function implemented in the program by varying the strain parameter. The cell parameter and the isotropic thermal parameters (B_{eq}) were refined with all atomic positions kept constant. For BSF, the initial atomic position of Bi^{3+} was set equal to the position of Sr^{2+} with occupancy factor of 0.5.

The oxygen nonstoichiometry and average valence of Fe in BSF and LSF were measured by iodometric titration. Approximately 0.1 g of powder was dissolved in a 6.0 mol l^{-1} HCl solution under argon atmosphere (to prevent the oxidation of I^- ions in air) before titration by thiosulfate ($S_2O_3^{2-}$) solution.

[†] Nanjing University of Technology
[‡] University of Queensland

Several drops of starch solutions were added to indicate the end points achieved when the initial transparent solution changed its color from orange to yellow.

For oxygen temperature programmed desorption (O_2-TPD), approximately 100 mg of the powders were loaded in a quartz tube. The tube was then placed in a tubular furnace equipped with a temperature controller. Argon at a flow rate of 20 ml min^{-1} (STP) was used as the carrier gas. The temperature was increased from 50 to 950°C at a ramp rate of 10°C min^{-1}. The effluent gases were monitored by a mass spectrometer (MS Hiden QIC-20).

The electrical conductivity relaxation (ECR) method was carried out to determine the oxygen bulk diffusion coefficient (D_{chem}) and surface exchange coefficient (k_{ex}). A 8mm×2mm×5mm BSF bar (previously sintered at 1050°C) was mechanically polished and cleaned (w/ ultrasonic treatment). The bar was heated in a furnace at a certain temperature under a controlled atmosphere. After a stabilization period, a sudden change in the oxygen partial pressure, e.g. 0.05 to 0.21 atm was introduced by sudden switching from initial gas to another gas. The conductivity as a function of time was measured using a four-probe DC method. The change in the oxygen partial pressure was achieved by mixing proportional amounts of argon and oxygen using mass flow controllers at a flow rate of 300 ml min^{-1} (STP). The test was performed between 800 and 600°C at an interval of 50°C. After each temperature change, the bar was stabilized for at least 1 h before data was collected. D_{chem} and k_{ex} were obtained by fitting the electrical conductivity relaxation curves with Equation (1).

$$g(t) = \frac{\sigma(t)-\sigma(0)}{\sigma(\infty)-\sigma(0)} = 1 - \sum_{n=1}^{\infty}\sum_{m=1}^{\infty}\sum_{p=1}^{\infty} \times \frac{2C_1^2 \exp(-\alpha_{1n}^2 D_{chem} t/l_1^2)}{\alpha_{1n}^2(\alpha_{1n}^2 + C_1^2 + C_1)} \times \frac{2C_2^2 \exp(-\alpha_{2m}^2 D_{chem} t/l_2^2)}{\alpha_{2m}^2(\alpha_{2m}^2 + C_2^2 + C_2)} \times \frac{2C_3^2 \exp(-\alpha_{3p}^2 D_{chem} t/l_3^2)}{\alpha_{3p}^2(\alpha_{3p}^2 + C_3^2 + C_3)} \quad (1)$$

Where σ(0), σ(t) and σ(∞) denotes the initial, time dependent and final conductivity, respectively. The parameters C_1, C_2 and C_3 are defined in Equation (2).

$$C_1 = \frac{l_1}{L_d} C_2 = \frac{l_2}{L_d} C_3 = \frac{l_3}{L_d} L_d = \frac{D_{chem}}{k_{ex}} \quad (2)$$

The coefficients α_{1n}, α_{2m} and α_{3p} are the roots of the transcendental equations as defined in Equation (3).

$$C_1 = \pm_{1n} \tan \pm_{1n} C_2 = \alpha_{2m} \tan \alpha_{2m} C_3 = \alpha_{3p} \tan \alpha_{3p} \quad (3)$$

The oxygen permeability measurement was performed using the gas chromatography (GC) method as detailed elsewhere.[3] Dense BSF or LSF disk were sealed onto the quartz tubes with silver paste. The circumferential surfaces of the disk were also covered with the sealant to avoid radial oxygen transport contribution. Helium at a flow rate of 100 ml min^{-1} was used as the sweep gas. The oxygen concentration on the permeate stream was analyzed using a gas chromatograph (Varian, CP 3800). The oxygen permeation flux ($J(O_2)$) was calculated using Equation (4).

$$J_L(O_2)\,(\mathrm{ml\ cm^{-2}\ min^{-1}, [STP]}) = (C_LO - C_LN \times 0.21)/(0.79 \times (28/32))^{0.5} \times Q/S \quad (4)$$

Where C_O and C_N are the measured concentration of oxygen and nitrogen, respectively in the permeate stream, respectively; Q is the flow rate of the permeate stream (ml min^{-1}) and S is effective area of the disk (cm^2).

The ionic conductivity was estimated using the Wagner relation shown as Equation (5) assuming that the bulk diffusion is the rate limiting step in 1-mm thick disk (confirmed in [4] for low Sr concentrations) and the electronic conductivity is substantially larger than the ionic conductivity.

$$J_{O_2} = \frac{RT\sigma_i}{16F^2L}\frac{\ln p_h}{P_l} \qquad (5)$$

Where R is the gas constant, T is the temperature, F is the Faraday constant, L is the thickness of the membrane and p_h and p_l are the partial oxygen pressures on the feed and permeate side, respectively. The oxygen concentration on the permeate stream (p_l) (measured by the GC) was used to estimate the oxygen partial pressure "driving force" for ionic conduction.

BSF slurry for spray deposition solution was prepared by dispersing BSF powder with a premixed solution of glycerol, ethylene glycol and isopropyl alcohol followed by rapid mixing and ball milling (Pulverisette 6, Fritsch) at 400 rpm for 0.5 hours.

Symmetrical cells of electrode|SDC|electrode configuration were fabricated by painting BSF slurry onto both surfaces of SDC disk in a symmetric configuration and calcining the painted cells at 1000°C for 2 hours in air.

A three-electrode setup was used to obtain the cathodic overpotential-current density curves. As a working electrode (WE), BSF slurry was painted on one side of SDC electrolyte disk to form an electrode area of 0.26 cm^2. Silver paste was painted symmetrically on the opposite side of the SDC disk as a counter electrode (CE). Silver paste was also painted in the circumferential surfaces of the disk as a reference electrode (RE).

The anode substrates were prepared by a tape casting process. The slurry for tape casting process was prepared by two step ball milling. NiO, YSZ and starch were ball milled with organic solvent in an agate jar for 24 h using triethanolamine as surfactant. Subsequently, polyvinyl butyral (PVB), and polyethylene glycol (PEG) and dibutyl o-phthalate (DOP) were added as binder and plasticizers respectively followed by ball milling for another 24h to form slurry. The slurry was vacuum pumped under 200 mbar (absolute) to remove air, and then cast onto the polymer carrier on a tape casting machine. The tape was dried in ambient condition for 24 h, and then detached from the polymer carrier. Circular anode substrate with a diameter of 16 mm was drilled from the tape by a punch followed by pre-sintering at 1150 ^oC in air to remove organic. The SDC|YSZ double electrolyte layers were prepared via wet powder spraying as described in Ref 5. The YSZ and SDC suspensions were sprayed onto the anode substrate in sequence using a spraying gun with a nozzle size of 0.35mm (diameter). Nitrogen was used as carrier gas at a working pressure of 1 atm. The spraying gun was aligned vertically to the anode substrate leaving a 10 mm distance between them. The spray speed was controlled at about 0.005 g (YSZ or SDC) s^{-1}. The spray process was carried out at a substrate temperature of ~200 ^oC with the help of a hot plate. After the spray deposition, the green triple-layer pellets were fired at 1450 ^oC in air for 5 h at a heating rate of 3 ^oC min^{-1}. BSF slurry was then painted onto the center of the disk electrolyte and fired at 1000^oC for 2 h in air. The resulting coin-shaped film cathode had a thickness of 10-20μm and an area of 0.48 cm^2.

The electrochemical impedance spectra (EIS) of the cells were obtained using an electrochemical workstation (Solartron 1260A frequency response analyzer and a Solartron 1287 potentiostat). The frequency range was 0.01 Hz to 100 kHz and the signal amplitude was 10 mV under open cell voltage conditions. Cathodic overpotential was measured using a Solartron 1287 potentiostat/galvanostat. The series resistance (IR) drop from the electrolyte and lead/contact resistances was also determined from the EIS data and subtracted to establish the IR free current-voltage characteristics.

Thermal expansion data were collected with a dilatometer (Netsch DIL 402C/3/G) from room temperature to 900^oC on a 2 mm × 5 mm × 12 mm BSF bar (previously sintered at 1050^oC in air).

BSF and LSF bars for conductivity testing were prepared by pressing the BSF and LSF powder into disk followed by sintering at 1050^oC and polishing into bar shape. Ag paste was painted on the square

cross-sectional edges and two circumferential surfaces of the bar to form the current and voltage electrodes. The electrical conductivities were measured by a four-probe DC technique using Keithley 2420 source meter at intervals of 5 ^{o}C within a temperature range of 300-900 ^{o}C.

Results

Table S1. Rietveld refinements results of BSF and LSF.

BSF							
Space group				Pm-3m			
PV_TCHZ peak type							
U				-0.24			
V				0.06			
W				-0.012			
Z				0			
X				0			
Y				0			
Lattice parameters							
a (Å)				3.94839			
Site	Np	x	y	z	Atom	Occupancy	B_{eq}
Bi	1	0.0000	0.0000	0.0000	Bi+3	0.5	3.90
Sr	1	0.0000	0.0000	0.0000	Sr+2	0.5	2.00
Fe	1	0.5000	0.5000	0.5000	Fe+3	1.0	0.77
O	3	0.5000	0.5000	0.0000	O-2	1.0	7.00
LSF							
Space group				R-3c			
PV_TCHZ peak type							
U				0			
V				-0.11			
W				0.011			
Z				0			
X				0			
Y				0			
Lattice parameters							
a (Å)				5.5180			
c (Å)				13.4462			
Site	Np	x	y	z	Atom	Occupancy	B_{eq}
La	6	0.0000	0.0000	0.2500	La+3	0.5	1.10
Sr	6	0.0000	0.0000	0.2500	Sr+2	0.5	2.00
Fe	6	0.0000	0.0000	0.0000	Fe+3	1.0	0.97
O	18	0.4651	0.0000	0.2500	O-2	1.0	3.44

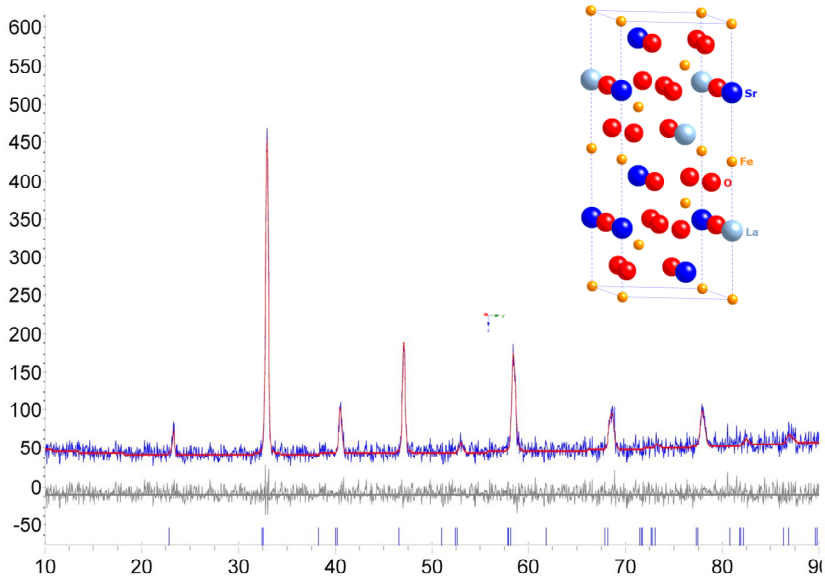

Figure S1. Rietveld refinement plot of LSF (Inset-Crystal structure of LSF).

Table S2. Oxygen nonstoichiometry and average valence of Fe in BSF and LSF

	Oxygen nonstoichiometry (δ)	Average valence of Fe
BSF	0.236	3.03
LSF	0.046	3.41

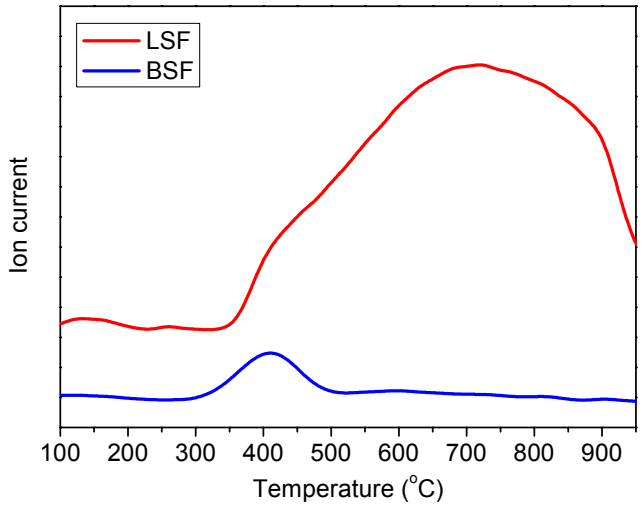

Figure S2. Oxygen temperature-programmed desorption (O_2-TPD) of BSF and LSF. The onset of oxygen desorption between 300 and 350°C for BSF and LSF is due to the reduction of Fe^{4+} to Fe^{3+}. The area of oxygen desorption is much smaller for BSF relative to LSF indicates very low amount of Fe^{4+} in BSF.

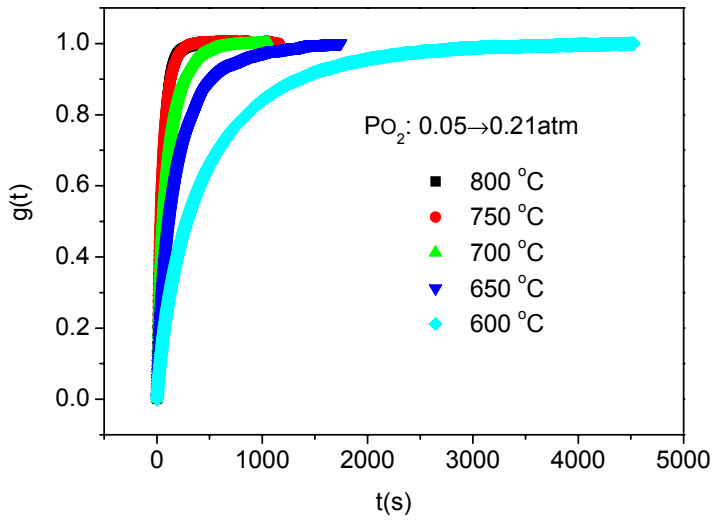

Figure S3. Electrical conductivity relaxation (ECR) response curves of BSF at various temperatures after sudden change of oxygen partial pressure from 0.05 to 0.21 atm.

Table S3. Oxygen fluxes and the calculated ionic conductivities of BSF and LSF.

BSF				
T (°C)	p_h (atm)	p_l (atm)	$J(O_2)$ (mol cm^{-2} s^{-1})	σ (S/cm)
800	0.21	4.69×10^{-4}	7.05×10^{-8}	0.01582
750	0.21	2.08×10^{-4}	3.13×10^{-8}	0.00649
700	0.21	1.31×10^{-4}	1.98×10^{-8}	0.00405
650	0.21	4.2×10^{-5}	6.32×10^{-9}	0.00118
600	0.21	8.710^{-6}	1.31×10^{-9}	0.00022
LSF				
800	0.21	6.68×10^{-5}	5.20×10^{-8}	0.00982
775	0.21	4.94×10^{-5}	3.85×10^{-8}	0.00717
750	0.21	3.55×10^{-5}	2.77×10^{-8}	0.00508
725	0.21	2.09×10^{-5}	1.63×10^{-8}	0.00289
700	0.21	1.26×10^{-5}	9.82×10^{-9}	0.00169

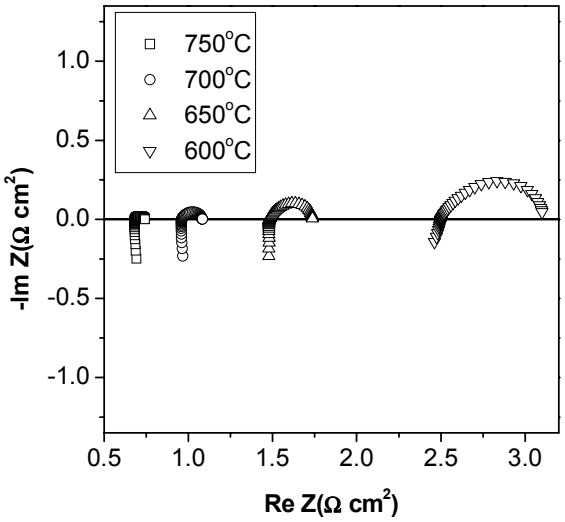

Figure S4. Electrochemical impedance spectra of BSF|SDC|BSF cell at 600-750°C in air.

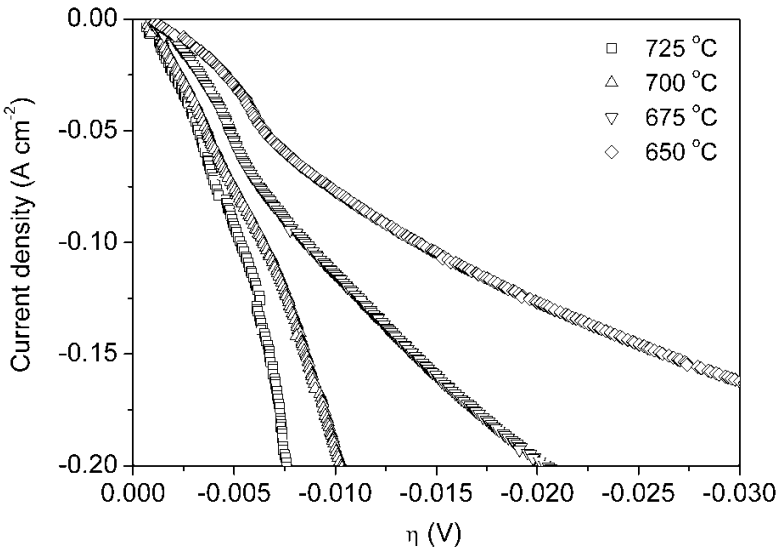

Figure S5. IR-corrected overpotential-current density plots as a function of temperature.

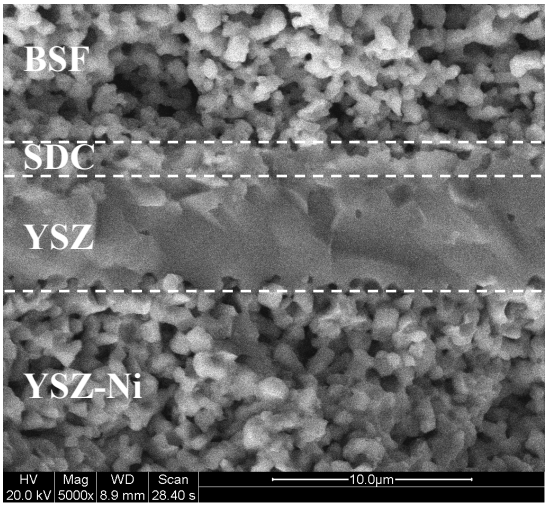

Figure S6. Scanning Electron Microscope (SEM) image of the cross-section of BSF|SDC|YSZ|YSZ-Ni cell.

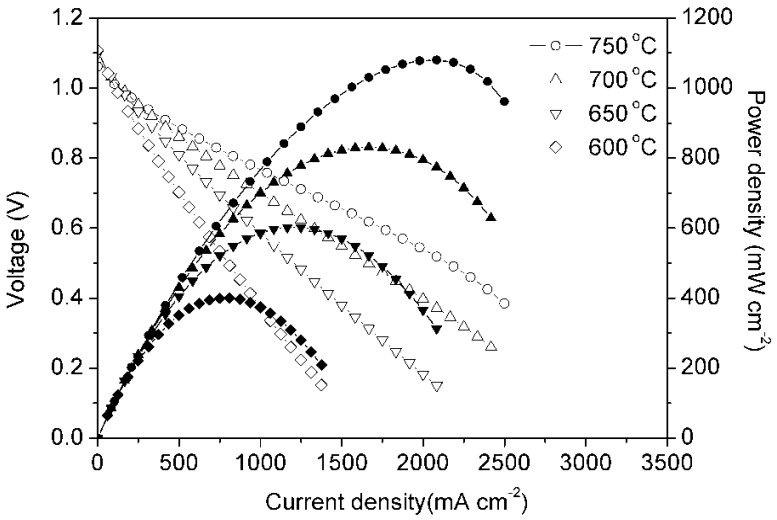

Figure S6. *I-V* and *I-P* curves of the complete cell based on a 8-µm thick SDC(2 µm)|YSZ(6 µm) electrolyte, BSCF cathode and a YSZ-Ni (50/50 vol%) anode.

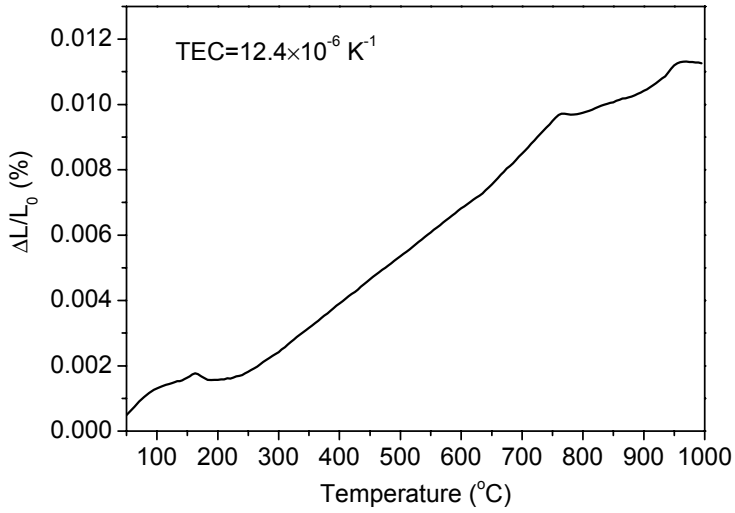

Figure S7. Thermal expansion curves of BSF.

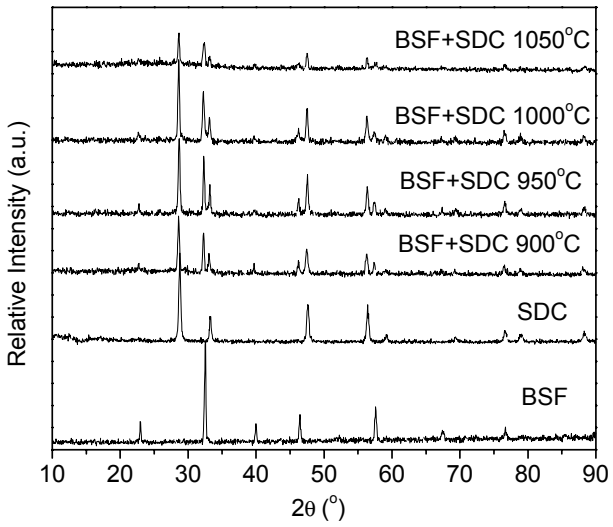

Figure S8. Phase reaction between BSF and SDC by mixing and firing them between 900-1050 °C for 2h

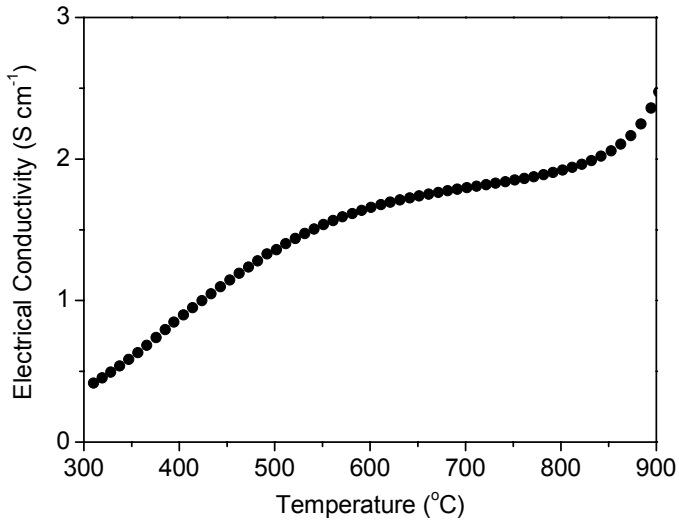

Figure S9. Electrical conductivity of BSF between 300-900 °C.

REFERENCES
(1) *DIFFRAC^{plus} TOPAS 4*; BrukerAXS GmbH: Karlsruhe, 2008.
(2) *Find-It: Inorganic Crystal Structure Database (ICSD)*; Fachinformationszentrum (FIZ): Karlsruhe, 2010.
(3) Sunarso, J.; Liu, S.; Lin, Y.S.; Diniz da Costa, J.C. *J. Membr. Sci.* **2009**, *344*, 281.
(4) Brinkman, K.; Iijima, T.; Takamura, H. *Jap. J. Appl. Phy.2* **2009**, *46*, L93.
(5) Zhou, W.; Shi, H.G.; Ran, R.; Cai, R.; Shao, Z.P.; Jin, W.Q. *J. Power Sources* **2008**, *184*, 229.